0026-895X/88/050551-08$02.00/0

MOLECULAR PHARMACOLOGY, 33:551-558

Interaction of the Antifolate Antibiotic Trimethoprim with Phosphatidylcholine Membranes: A ^{13}C and ^{31}P Nuclear Magnetic Resonance Study

GEORGE R. PAINTER, RON GRUNWALD, and BARBARA ROTH
The Wellcome Research Laboratories, Research Triangle Park, North Carolina 27709
Received September 1, 1987; Accepted February 2, 1988

SUMMARY

The interaction of the bacterial dihydrofolate reductase inhibitor trimethoprim with small unilamellar 1,2-dimyristoyl-*sn*-glycero-3-phosphorylcholine vesicles was studied using ^{13}C and ^{31}P NMR spectroscopy. In an effort to determine whether trimethoprim passively permeates the vesicle membrane, an impermeant, anionic complex of the paramagnetic ion Dy^{3+} was added to the extravesicular compartment. Based on the downfield shift that the Dy^{3+} complex induces in the [2-^{13}C] resonance of trimethoprim in free solution, membrane permeation and movement of the drug into the intravesicular space can in principle be established from observation of the C2 chemical shift alone. In contrast to what is predicted by a two-compartment model separated by a semipermeable barrier, the presence of vesicles virtually reverses the effect of the shift reagent on the [2-^{13}C] carbon resonance. These results suggest that the majority of the trimethoprim might be sequestered within the vesicle membrane. A saturable decrease in the spin-lattice relaxation time and a saturable increase in the line width at half-height of the [2-^{13}C] resonance as a function of vesicle concentration indicated that trimethoprim does in fact bind to the phospholipid matrix of the membrane bilayer. The K_D for the interaction calculated from the relaxation data was $9.7 \pm 0.3 \times 10^{-4}$ M at a pH of 7.01 and an ionic strength of 0.015 M. The chemical shift of the [2-^{13}C] resonance is unaffected by interaction with the electroneutral membrane, and the pK_a increases by only 0.16 upon binding. These results point to an interfacial location for the pyrimidine moiety. Using the paramagnetic shift reagent Pr^{3+} and the ^{31}P NMR signal from the phosphodiester groups of the membrane lipids, trimethoprim was shown to displace Pr^{3+} ions from binding sites on the outer membrane surface as would be expected if the polar pyrimidine ring were located at or near the membrane surface. The extent to which trimethoprim and trimethoprim derivatives modified in the 3′- and 4′-positions interact with the *exo* face of the membrane is strongly dependent on the type of substituent and whether it is in the 3′- or 4′-position. Van der Waals interactions between the 5-benzyl sidechain and the hydrophobic fatty acid region of the membrane interior appear to be necessary for the polar portion of trimethoprim to compete favorably for the membrane-binding site with the polyvalent Pr^{3+} ion. Attempts to displace Pr^{3+} bound to the *endo* face of the vesicle membrane with trimethoprim or more lipophilic derivatives of trimethoprim were unsuccessful, indicating that the drug will not passively diffuse across the vesicle membrane. This inability to permeate the membrane is attributed to the high energy required to break hydrogen bonds between the hydrogen bond donors and acceptors on the 2,4-diaminopyrimidine ring and extravesicular water at the membrane interface.

The cytoplasmic enzyme DHFR (EC 1.5.1.3) is the target for folate antagonists such as the antineoplastic 2,4-diaminopteridine, methotrexate (1), and the antimicrobial 2,4-diaminopyrimidine, TMP (2) (Fig. 1). The mechanism of delivery to the active site figures significantly in the observed cytotoxicity of both classes of drugs. Methotrexate enters a number of different cell types, with varying degrees of efficiency, by a facilitated process in which endogenous folate and tetrahydrofolate transport proteins are utilized as carriers (3). In L1210 murine leukemia cells, for example, methotrexate uptake exhibits Michaelis-Menten kinetics with competitive inhibition by folate analogs and a high degree of structural specificity (4). The inhibition of 5,6-disubstituted 2,4-diaminopyrimidine uptake in L5178Y lymphoblasts by folinic acid (5) and the apparent competitive inhibition of methotrexate uptake in W1-L2 human lymphoblastoid cells by TMP (6) indicate that the pyrimidine class of DHFR inhibitors can also utilize the folate carrier protein. However, the mechanism(s) of 2,4-diaminopteridine and 2,4-diaminopyrimidine transport in systems lacking appropriate carrier proteins (such as Gram-negative bacteria and transport-deficient mammalian cell lines) is (are) equivocal.

Studies of the cellular uptake of the 5,6-disubstituted 2,4-

ABBREVIATIONS: DHFR, dihydrofolate reductase; TMP, trimethoprim; DDMP, 2,4-diamino-5-(3′,4′-dichlorophenyl)-6-methylpyrimidine; DDEP, 2,4-diamino-5-(3′,4′-dichlorophenyl)-6-ethylpyrimidine; DAMP, 2,4-diamino-5-adamantyl-6-methylpyrimidine; EDTA, ethylenediaminetetraacetate; DTPA, diethylenetriaminepentaacetate; NTA, nitrilotriacetate; TTHA, triethylenetetramine hexaacetate; DMPC, 1,2-dimyristoyl-*sn*-glycero-3-phosphoryl choline; OMe, 3′-*O-methyl*; HEPES, *N*-2-hydroxyethylpiperazine-*N*′-2-ethanesulfonic acid; SUV, small unilamellar vesicle; LIS, lanthanide-induced shift; TAP, 2,4,6-triaminopyrimidine; cp, centipoise.

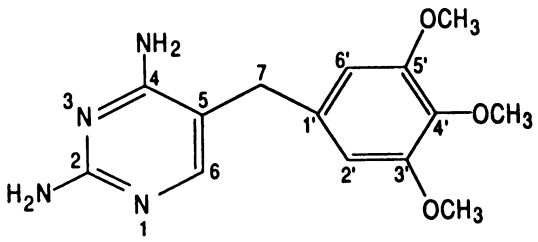

Fig. 1. Structure of TMP [2,4-diamino-5-(3′,4′,5′-trimethoxybenzyl)pyrimidine].

diaminopyrimidines DDMP, DDEP, and DAMP in methotrexate-resistant Hep-2 and KB human cell lines have found transport of the drugs to be unaffected by temperature, metabolic inhibitors, or the presence of folate analogs (7). At equilibrium the intracellular concentration of each drug is 2–3 orders of magnitude greater than the extracellular concentration, presumably due to extensive nonspecific binding to intracellular protein. Saturation kinetics observed in the transport experiments were explained by saturation of the intracellular binding sites rather than saturation of a transmembrane carrier. A positive correlation was found between the lipophilicity of the three compounds and the extent of uptake and growth inhibition.

In contrast, increasing the lipophilicity of TMP by derivatization of the 5-(3′,4′,5′-trimethoxybenzyl) moiety consistently results in a *decrease* in overall *in vitro* activity in gram negative bacteria even though the I_{50} of the derivatives measured against isolated *Escherichia coli* DHFR is comparable to or less than that of the parent TMP (8). Cellular fractionation studies done on *E. coli* indicate that, unlike the more lipophilic 5,6-disubstituted diaminopyrimidines, TMP tends to concentrate in the membrane fraction and does not show the same propensity to partition into the intracellular compartment.[1]

Lack of understanding of the mechanism by which TMP interacts with and crosses biological membranes has severely hampered efforts to design rationally a TMP analog with increased *in vitro* activity. As a first step in determining the physicochemical factors regulating the interactions of 5-benzyl 2,4-diaminopyrimidines with biomembranes, ^{13}C and ^{31}P NMR techniques were used to investigate the interactions of TMP and TMP derivatives with DMPC vesicle membranes. The vesicle membrane is generally accepted as an adequate model of the phospholipid matrix of the biological membrane through which the drug must pass if it reaches DHFR in the intracellular space by passive diffusion (9). NMR spectroscopy has proven extremely useful for the study of weak, reversible interactions between small molecules and macromolecules or large molecular aggregates (10). The information on the manner of binding and dynamic features of the drug in the membrane bilayer obtainable with NMR is of primary importance in developing an understanding of the influence of the structural features of the drug on membrane permeability and, ultimately, in determining what modifications can be made to the drug to ensure a higher degree of chemical activity in the intracellular space.

Materials and Methods

Reagents. TMP was manufactured by The Burroughs Wellcome Co. [2-^{13}C]TMP was synthesized by condensation of [^{13}C]guanidine (90% enrichment; U.S. Services Inc.) with β-anilino-α-(3,4,5-trimethoxybenzyl)acrylonitrile (11). The 3′- and 4′-substituted derivatives of TMP were synthesized by previously published procedures (8). Praseodymium, europium, dysprosium, lanthanum, and thulium (Aldrich, 99%) were purchased as chloride salts and used without further purification. EDTA, DTPA, NTA, and TTHA (Aldrich, 98–99%) were used as the free acids without further purification. Shift reagent complexes were prepared by dissolving the appropriate lanthanide and chelator in aqueous HEPES buffer and adjusting the pH to neutrality with tetraethylammonium hydroxide (Alfa, 40% aqueous). DMPC was obtained from Avanti Polar Lipids and used without further purification.

Preparation of phospholipid vesicles. Aliquots of a 20 mg/ml chloroform solution of DMPC were dried on a rotary evaporator and vacuum desiccated for 12 h. The lipids (100–150 mg) were resuspended in 2–3 ml of an aqueous solution containing 1 mM EDTA and 10 mM HEPES at a pH of 7.0 and sonicated in a Heat Systems W-375 sonicator with a cuphorn attachment to form SUVs. The sonicated lipids were centrifuged at 100,000 × *g* for 30 min to pellet any large multilamellar vesicles. EDTA was eliminated from experiments in which lanthanides were added to the vesicle preparation. Praseodymium-loaded vesicles were prepared by sonication in the presence of 2 mM $PrCl_3$ followed by dialysis for 2 hr in a buffer solution containing 2 mM $LaCl_3$. All experiments were carried out above the gel-to-liquid crystal phase transition temperature of DMPC at 25.7°. The concentration of DMPC in each sample was determined as inorganic phosphate by a modification of the method of Ames and Dubin (12).

NMR spectroscopy. All NMR spectra were run on a Varian XL-300 NMR spectrometer operating in the pulsed Fourier transform mode in a 10-mm broadband tunable probe at 25.7°. Observation frequencies were 75.43 MHz for ^{13}C and 121.42 MHz for ^{31}P. Standard ^{13}C and ^{31}P spectra were accumulated with WALTZ decoupling (13). ^{13}C chemical shifts are reported relative to external dioxane and ^{31}P chemical shifts are reported relative to external 85% phosphoric acid. The spin-lattice relaxation times (T_1 values) for the [2-^{13}C] carbon of TMP were measured as a function of DMPC concentration from partially relaxed spectra obtained using a $(\pi\text{-}t\text{-}\pi/2T)_n$ pulse sequence (14). The repetition rate, T, was set to 5 times the estimated T_1. Each determination included a minimum of 10 incremental relaxation delay times, t, ranging from 0.4 to 1.5 T_1. Results were analyzed using a two-parameter fit procedure that included a B_1 inhomogeneity factor (15). The magnitude of the ^{13}C-[^1H] nuclear Overhauser effect was determined from the difference in integrated intensity observed for the ^{13}C resonances in ^1H noise decoupling and ^1H gated decoupling experiments.

Viscosity determination. The viscosity of a series of DMPC vesicle solutions (0.5 mM TMP, 10 mM tetraethylammonium HEPES, 1 mM EDTA, pH 7.0, 25.7°) was determined over a 0–130 mM DMPC concentration range using the procedure described by Cory *et al.* (16). Measurements were made on a Cannon-Ubbelhode semi-microdilution viscometer (series 75, Cannon Instrument Co.) maintained at 25.7° by a Cannon constant temperature bath. Flow times, t, were measured in triplicate using a hand-held stopwatch and were found to have an average error of less than 1%. Viscosity in centipoise was calculated from measured t values using the expression

$$\eta = A\ d\ t$$

where d is the measured density of the solution at 25.7° and A is the empirically determined viscometer constant (0.009266 centistokes sec^{-1} for the apparatus used in this study).

Results and Discussion

The ability of TMP to distribute across the lipid bilayer of SUVs made from DMPC was investigated as a simple model of TMP permeation in biological membranes. Addition of impermeant complexes of paramagnetic ions to the medium in which the DMPC SUVs are suspended renders the intra- and extra-

[1] Personal communication from Dr. Paul Ray, Department of Microbiology, Burroughs Wellcome Co., Research Triangle Park, NC.

vesicular compartments anisochronous, and under appropriate conditions allows the distribution of a compound across the membrane barrier to be determined by examination of NMR chemical shifts (17). If the permeant compound were in slow transmembrane exchange, two sets of NMR signals would be observed corresponding to the populations inside and outside the vesicle. The population proximal to the lanthanide shift reagent (in the extravesicular space) would be shifted relative to the signal from the fraction sequestered in the vesicle interior. The magnitude and direction of the LIS depends upon the particular lanthanide complex used and the strength and geometry of its interaction with the molecule under investigation. If transmembrane movement of the permeant molecule is fast on the NMR time scale, then a single set of NMR resonances should be observed whose chemical shifts are the population weighted averages of the chemical shifts of the compound in the presence and absence of the shift reagent. The LIS technique has been used to differentiate between metal ions in the inner and outer compartments of phospholipid vesicles (18) and, provided a suitable shift reagent can be identified, can in principle be used to differentiate between TMP in the inner and outer compartments of DMPC vesicles.

In general, an LIS results from a combination of contact, pseudocontact, and complex formation terms (19). In the case of trimethoprim, a pseudocontact interaction might be expected between the lanthanide shift reagent and the N1 and/or N3 pyrimidyl nitrogens and the C2 and C4 amino groups. Such an interaction would be expected to produce substantial chemical shifts in the ^{13}C resonances of the carbon atoms in the pyrimidine ring. Water-soluble TAP was used as a model of the pyrimidine ring of TMP in an effort to identify a shift reagent that produces suitable LISs. TAP has a pK_a close to that of TMP.

The effects of the hexaquo complexes of the paramagnetic ions Dy^{3+}, Tm^{3+}, Eu^{3+}, and Pr^{3+} on the ^{13}C chemical shifts of TAP were examined first. These complexes proved to be poor shift reagents for TAP, presumably due to the inability of the pyrimidine nitrogen atoms to compete with water molecules as first coordination sphere ligands. Lanthanides show a distinct preference for hard Lewis bases, such as oxygen, as first coordination sphere ligands (20). In addition, TAP is partially protonated at the N1 position at pH 7.0. Therefore, charge-charge repulsion might contribute to the lack of interaction. Anionic complexes of the paramagnetic ions proved to be more effective shift reagents for TAP. The Dy^{3+}, Tm^{3+}, Eu^{3+}, and Pr^{3+} ions were examined as their TTHA, $(NTA)_2$, DTPA, and EDTA complexes. The magnitude of the LIS induced by the complexes followed the trend $Dy^{3+} \geq Tm^{3+} \gg Eu^{3+} \geq Pr^{3+}$ for any one chelate. For any lanthanide the magnitude of the LIS followed the trend LnTTHA>$Ln(NTA)_2$>Ln-DPTA>LnEDTA. Fig. 2A shows the effects of DyTTHA, DyEDTA, and DyDTPA on the chemical shifts of the carbon atoms of TAP. DyTTHA is the most efficacious shift reagent. The largest effect is observed at the C2 position, with the effect decreasing in the order C2 > C4 = C6 > C5. The DyTTHA complex was also extremely effective in shifting the C2 resonance of TMP (Fig. 2B). In addition, the observed shift of the C2 resonance of TMP increases as the pH is decreased from 8.0 to 6.0, as would be expected if ion pairing between the anionic shift reagent and the N1 protonated pyrimidine ring (pK_a 6.54 ± 0.01) is important in the intermolecular interaction. Such an interaction has been observed between the positively charged center of nicotine *N*-methiodide and anionic lanthanide shift reagents (22). There is no effect observed at the 3′-position of TMP, suggesting that the interaction is confined to the pyrimidine ring (Fig. 2B).

The [2-^{13}C] resonance of 1 mM TMP in aqueous buffer undergoes a 180-Hz downfield LIS from 160.09 ppm to 162.49 ppm in the presence of 8 mM DyTTHA. The use of TMP 90% labeled in the C2 position allows rapid accumulation of shift data in aqueous media and, in experiments involving vesicles, permits drug levels to be kept well below concentrations at which significant disruption of vesicle membrane organization might occur. In a 50 mM solution of DMPC SUVs, the downfield chemical shift induced by 8 mM DyTTHA is reduced to 30 Hz. The presence of SUVs virtually reverses the effect of the lanthanide shift reagent. Assuming an average vesicular diameter of 300 Å, a bilayer thickness of 40 Å, and an aggregation number of 2500, the intravesicular volume of a 50 mM DMPC solution is approximately 10% of the total available volume (23). Consequently, if TMP had equilibrated across the vesicular membrane, approximately 10% of the drug would be within the intravesicular space at any given time. Under the condition of slow exchange between the inner and outer compartments, a peak corresponding to TMP in the intravesicular space would be expected to appear 180 Hz downfield from and integrable for 10% of the area of the peak corresponding to the TMP remaining in the large extravesicular compartment. If the TMP was in fast exchange between the two compartments, a single resonance would be observed 162 Hz downfield of the position observed in the absence of the shift reagent. The extreme diminution of the LIS upon addition of SUVs is not consistent with a simple model consisting of two aqueous compartments separated by a semipermeable barrier. Binding of the shift reagent to the surface of the vesicle where it becomes inaccessible to the TMP can be ruled out since the ^{13}C resonances of the choline head groups of the bilayer lipids are not shifted in the presence of DyTTHA. One possible explanation for the loss of effect of DyTTHA on the TMP signal is that the majority of the TMP binds to the vesicular membrane and is consequently isolated from the shift reagent.

The binding of small molecules to a macromolecule (10) or to a large molecular aggregate (24) often results in decreased T_1 values and enhanced NMR linewidths ($\Delta\nu_{1/2}$) of one or more resonances of the ligand. These changes are primarily the result of a decrease in the Brownian motion of the small molecule in the bound state and/or an increase in the number of magnetic neighbors (25). Fig. 3 shows the effect of increasing concentrations of DMPC on the observed T_1 of the [2-^{13}C] resonance of a 0.5 mM solution of TMP. The T_1 decreases with increasing DMPC up to a lipid-to-drug ratio of 64:1. Changes in $\Delta\nu_{1/2}$ as a function of increasing DMPC concentration parallel the observed changes in T_1 (Table 1). Lipid-to-drug ratios greater than 64:1 produce no further change in either parameter.

To ensure that the observed changes are not simply the result of nonspecific motional attenuation arising from increases in solution viscosity, the viscosity of each DMPC solution was measured and the expected effect of viscosity on the T_1 values calculated. Because, in a given solution, at constant temperature, T_1 will vary inversely with η, where η is the measured viscosity, the T_1 change expected from a change in η can be calculated using the ratio

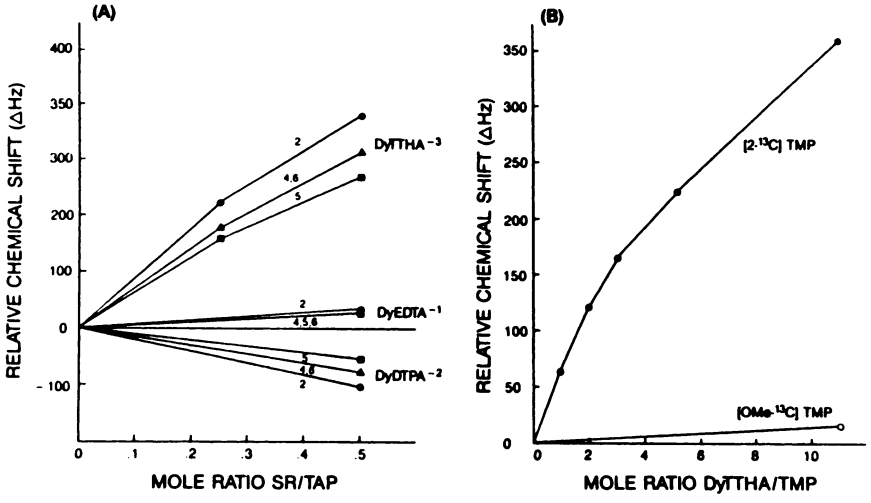

Fig. 2. A. Anionic Dy^{3+} complex-induced shifts in the 2C (●), 4 and 6C (▲), and 5c (■) ^{13}C resonances of a 65 mM aqueous solution of TAP at 25°. The relative chemical shifts (ΔHz) are calculated as the differences in chemical shifts observed in the presence of the Dy^{3+} complex and the analogous La^{3+} complex. *tert*-Butyl alcohol (0.15%), which has been shown to exhibit no contact or pseudocontact shifts with the complexes used (21), was utilized as an internal standard. Solutions were made in D_2O and adjusted to pH* 6.6 with tetraethylammonium hydroxide. Tetraethylammonium was used as a counterion since it was demonstrated to have no appreciable interaction with the shift reagents. B. DyTTHA-induced shifts in the [2-^{13}C] and [3′-O Methyl] resonances of a 1 mM aqueous solution of TMP. Both the [2-^{13}C] and [OMe] positions were 90% ^{13}C enriched. The relative chemical shift was calculated as in A for 0–10 mM DyTTHA. The D_2O solutions were buffered with 20 mM tetraethylammonium-HEPES and adjusted to pH* 6.6.

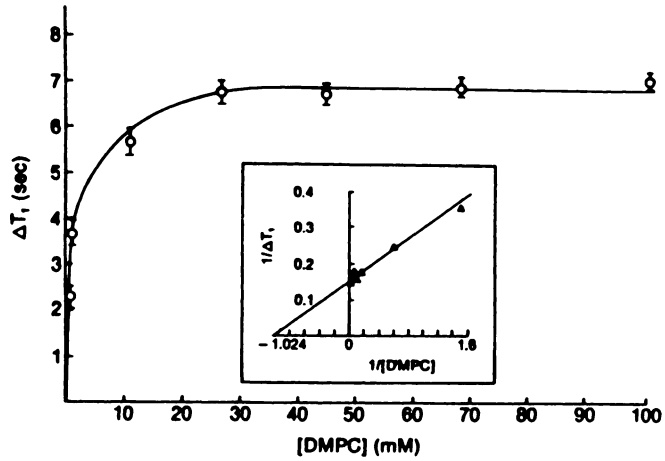

Fig. 3. A plot of the change in spin-lattice relaxation time (ΔT_1) of the [2-^{13}C]resonance of TMP in buffer at a pH of 7.0, an ionic strength of 0.015 M, and 25.7° as a function of DMPC concentration. The resonance appears at 93.5 ppm. Each point represents the average of from three to five independent determinations ± standard error. Typical ^{13}C acquisition parameters for the inversion-recovery experiment are: spectral window, 4.3 kHz: 90° pulse width, 18.6 μsec; delay between pulses, 10.8 to 46 sec T_1: 600 accumulations.

TABLE 1

Observed T_1 and $\Delta\nu_{1/2}$ values for 0.5 mM TMP in DMPC vesicle dispersions, and calculated T_1 values, T_1 calc, expected from changes in solution viscosity η

DMPC	T_1	$\Delta\nu_{1/2}$	η	T_1 calc
mM	*sec*	*Hz*	*cp*	*sec*
0	9.21	2.16	0.8705	9.21
0.69	6.34	5.52	0.8732	9.18
1.64	5.09	7.98	0.8769	9.14
11.42	3.53	10.59	0.9150	8.76
28.48	2.42	11.46	0.9815	8.17
44.61	2.51	11.62	1.0483	7.68
68.47	2.37	11.38	1.1370	7.09
99.89	2.17	11.81	1.2261	6.58

$$(T_1)_1/(T_1)_2 = \eta_2/\eta_1 \quad (1)$$

Application of Eq. 1 is straightforward when the observed carbon atom relaxes via a dipole-dipole relaxation mechanism (26). In both the presence and absence of DMPC, the contribution of dipole-dipole relaxation to the total relaxation mechanism of the atom is greater than 90% as evidenced by 91% nOe in the absence of vesicles and 94% in the presence of vesicles. Measured viscosities and T_1 values calculated using Eq. 1, T_1calc, over the range of DMPC concentrations used in the study are shown in Table 1. The increase in viscosity was linear over the range of 0–100 mM DMPC (η = 0.003899 cp/mM [DMPC] + 0.8705 cp, r^2 = 0.9934) and, as a result, T_1calc decreases linearly from the value of 9.21 sec observed in buffer to 6.58 sec at 100 mM DMPC. Over the range of 0–32 mM DMPC, where the maximal change in T_1 is observed, the expected decrease due to viscosity alone would be from 9.21 sec to the T_1calc value of 8.13 sec. The change in T_1 as a function of [DMPC] is in great excess of the effect predicted from viscosity and is saturable, showing no further increase above 32 mM DMPC, suggesting that the binding of a fraction of the TMP molecules is responsible for the relaxation effects.

At a fixed concentration of DMPC, increasing the TMP-to-DMPC ratio results in decreased linewidths and increased T_1 values, in accord with the system being in fast exchange between the free and bound form of the drug, i.e., a reversible binding obeying the law of mass action (10). Under these conditions, the relaxation data can be used to obtain the apparent K_D value for the interaction between TMP and DMPC. The K_D calculated from an unweighted nonlinear regression analysis of the saturation isotherm in Fig. 2 is $9.8 \pm 0.3 \times 10^{-4}$ M. The linearity of the double reciprocal plot of these data (see *Inset*, Fig. 3) suggests that the binding of the drug to the vesicle membrane can be adequately described by the following equilibrium:

$$(\text{TMP})_{\text{free}} + (\text{DMPC}) \rightleftharpoons (\text{TMP})_{\text{bound}}$$

The K_D can only be considered an apparent dissociation constant in that it does not take into account the stoichiometry of the phospholipid/TMP interaction.

The ^{13}C chemical shift at the 2-position is a sensitive indicator of the protonation state of the 2,4-diaminopyrimidine ring of TMP (27). An increase or decrease in the mole fraction of N1 protonated TMP produces a proportional upfield or downfield shift of the [2-^{13}C] resonance. An upfield shift observed for this resonance in the presence of DHFR has been interpreted as indicating that TMP binds preferentially to the enzyme in the N1 protonated form (27). If the association of TMP with phospholipid membranes involves an electrostatic

interaction analogous to that observed with DHFR, then the N1 protonated TMP could form a hydrogen-bonded ion pair with the phosphodiester linkage of the DMPC. Indeed guanidyl moieties show a strong propensity to interact electrostatically with negatively charged phosphate groups (28). However, in contrast to TMP binding to DHFR, the chemical shift of the [2-^{13}C] resonance is invariant during the DMPC titration, indicating that (i) the magnetic environments in solution and at the membrane-binding site are similar, and (ii) there is no significant shift in the protonation equilibrium of TMP associated with membrane binding.

The pK_a of membrane-bound TMP was calculated from the pH dependence of the chemical shift of the [2-^{13}C] resonance and found to be 6.71 ± 0.05, slightly less than the value of 6.54 ± 0.01 measured in free solution (29). Given the usual polarity dependence of apparent pK_a values, the 2,4-diaminopyrimidine ring cannot be buried deep in the apolar membrane interior but must be located in a high polarity microenvironment near the membrane surface.

The interfacial location of a molecule can often be determined from changes in the ^{31}P NMR spectrum of the membrane due to perturbation of lipid headgroup conformation or, in the case of polar molecules, by the displacement of ions bound to the membrane surface (30). The reversal of paramagnetic lanthanide ion-induced separation of the *endo* and *exo* face ^{31}P signals of vesicle membranes has been used to evaluate quantitatively the interaction of various drugs with the *exo* face of the vesicle (31). Since the ions bind strongly to, but do not permeate, the membrane, addition of Pr^{3+} to a vesicle suspension results in the magnetic properties of the ^{31}P atoms on the *exo* face being selectively modified. As a result, the ^{31}P signal from the outward-facing lipids is shifted downfield relative to that of the inward-facing lipids (Fig. 4A). The interaction of the ammonium group of the anesthetic tetracaine with the polar regions of the *exo* face of the membrane bilayer, for example, has been detected by a cancelling out of the Pr^{3+}-induced differentiation shifts in choline ^{1}H resonances. The ammonium group moves into and displaces Pr^{3+} ions from the ion-binding site on the membrane surface (32).

Localization of the hydrophilic 2,4-diaminopyrimidine moiety of TMP in the polar regions near the membrane surface might also be expected to result in the displacement of membrane-bound Pr^{3+}. We found that TMP effectively reverses Pr^{3+}-induced splitting of the membrane ^{31}P signal, producing half-maximal ion displacement at $1.26 \pm 0.09 \times 10^{-3}$ M under experimental conditions described in Fig. 4B. Fig. 4B illustrates a titration of Pr^{3+}-treated membranes with the 4′-$O(CH_2)_3SCH_2C_6H_6$ derivative of TMP (see below). As the concentration of the drug in the lipid dispersion is increased, the lowfield *exo* ^{31}P resonance shifts upfield toward the resonance position observed in the absence of paramagnetic ions.

The displacement of Pr^{3+} at the membrane surface by organic molecules requires a hydrophobic interaction in addition to the positioning of a polar functionality at the interface (33). The molecule must possess a group that can penetrate into the bilayer interior and anchor the molecule into the membrane via van der Waals forces. This interaction enables the polar portion of the molecule to compete favorably with the polyvalent cation for the binding site formed by the lipid phosphates. The geometry of the molecule must be such that both the hydrophilic and hydrophobic moieties can simultaneously interact in a favorable fashion with the appropriate regions of the membrane bilayer. The effectiveness of various lipophilic derivatives of TMP in displacing membrane-bound Pr^{3+} is shown in Table 2. It is apparent that simple models of the polar pyrimidine ring of TMP, such as guanidine and TAP, are relatively ineffective at displacing Pr^{3+} when compared to TMP. The lipophilic 5-benzyl substituent is necessary for a high degree of activity. Increasing the lipophilicity of the 5-benzyl group by substitution of more elaborate functionality in the 3′- or 4′-position increases the efficacy of Pr^{3+} displacement. Displacement ability is not, however, a strict function of lipophilicity as indicated by the lack of correlation between relative displacement efficacy and calculated log P (*C* log *P*). The 4′-allyloxy derivative, for example, has the lowest *C* log *P* value but the highest relative displacement capacity. Based on lipophilic properties alone, this is unexpected, since the other derivatives potentially possess larger hydrophobic surface areas for van der Waals interactions with the membrane lipids.

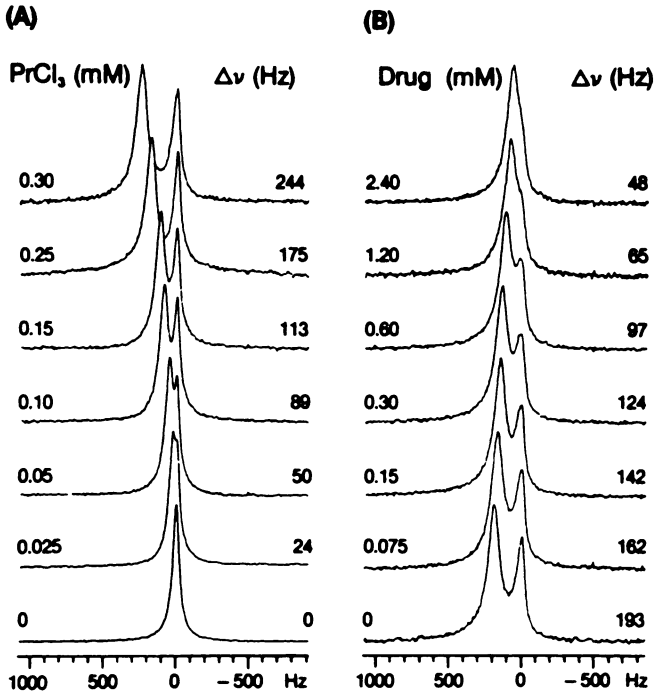

Fig. 4. A. The chemical shift separation (Hz) of the ^{31}P signals of inward- and outward-facing phosphodiester groups of a sonicated aqueous dispersions of DMPC as a function of $PrCl_3$ concentration. The titrations were conducted at 25.7°. Aliquots of a 50 mM solution of $PrCl_3$ were added to 2 ml of an 18 mM solution of sonicated DMPC. The pH was maintained at 7.0 throughout the titration. B. The reversal of Pr^{3+}-induced splitting of the DMPC ^{31}P signal by the 4′-($O(CH_2)_3SCH_2C_6H_5$) derivative of TMP. The drug, 300 mM in dimethyl sulfoxide, was added to a solution of DMPC containing 0.45 mM Pr^{3+}. Typical ^{31}P acquisition parameters are: spectral window, 5 kHz; 90° pulse width, 12 μsec; delay between pulses, 2 sec; 100–300 accumulations.

In all cases, the 4′-substituted compounds interact more favorably with the membrane than do their corresponding 3′-isomers. The origin of this effect may be steric. Location of the pyrimidine ring near the phosphodiester site of Pr^{3+} binding places the benzyl group just below the glycerol backbone region of the membrane bilayer (see Fig. 5). Tight intermolecular packing occurs in this region; therefore, molecules having a lower volume requirement for insertion into the phospholipid matrix would be expected to interact more favorably. The

TABLE 2

Relative efficiency of Pr^{3+} displacement from the exo face of DMPC vesicles, calculated lipophilicity (C log P), and number of conformational options (W) of TMP and TMP derivatives

Compound	Relative efficacy of Pr^{3+} displacement[a]	C Log P[b]	W[c]
Guanidine	0.19	−1.701	
2,4,6-Triaminopyrimidine	0.62	−0.058	
TMP	1.00	0.961	66
TMP-3′-(-O$(CH_2)_3$Cl)	1.22	1.731	702
TMP-4′-(O$(CH_2)_3$Cl)	2.10	1.731	720
TMP-3′-(-O$(CH_2)_3SCH_2C_6H_5$)	1.08	3.405	2494
TMP-4′-(-O$(CH_2)_3SCH_2C_6H_5$)	1.99	3.405	2640
TMP-3′-(O$CH_2CH{=}CH_2$)	4.19	1.474	450
TMP-4′-(O$CH_2CH{=}CH_2$)	9.23	1.474	354

[a] The relative displacement efficacy of each compound was calculated as the initial slope of the $PrCl_3$ titration curve normalized to the initial slope of the TMP displacement curve. The initial slopes were calculated as the ratio $\Delta\nu_{max}/K_{\nu_2}$, where $\Delta\nu_{max}$ is the maximal change in the ^{31}P resonance splitting and K_{ν_2} is the concentration of drug required to induce half-maximal change. Both $\Delta\nu_{max}$ and K_{ν_2} were derived from a nonlinear regression analysis of the titration data using a single component hyperbolic (saturable) binding model.

[b] C Log P values were calculated using MedChem software available from the Medicinal Chemistry Project, Pomona College, Clairmont, CA.

[c] The number of conformational options available to each TMP derivative was calculated using the internal coordinate conformer generator MVLTIC as a submode of the iterative molecular modeling program MACROMODEL.[2] A cutoff distance of 3 Å was used to eliminate conformers having severe nonbonded interactions.

[2] The molecular model was created using the program MACROMODEL, developed by W. Guida and N. Richards, Department of Chemistry, Columbia University, New York, NY.

benzylic ring of TMP rotates on an axis extending from C7 to C4′ (27). Substitution at the 4′-position places the substituent on this axis, thereby inducing a minimal increase in the volume swept out by the rotating benzylic side chain. However, substitution at the 3′-position places the substituent approximately 60° off the rotational axis and results in a substantially larger molecular volume being swept in space by the rotating ring. Thus, we would expect a higher energy cost for intercalation of the 3′-isomers.

The transbilayer diffusion of TMP can be gauged by the extent of its interaction with the internal surface of the vesicle. Movement of the drug across the membrane bilayer of vesicles loaded with Pr^{3+} and equilibration with a binding site on the *endo* face, analogous to the ionic binding site on the *exo* face, would result in the displacement of Pr^{3+} from the *endo* face. The transbilayer permeation of chlorpromazine in lecithin vesicles has been detected by the reversal of Pr^{3+}-induced shifts of the ^1H NMR signal of the *endo* choline methyls (34). Encapsulation of 2 mM Pr^{3+} induces a 180.6-Hz downfield shift of the ^{31}P resonance of the *endo* phosphodiester group. The Pr^{3+}-loaded vesicles were titrated with TMP to a final concentration of 5 mM, twice the concentration required to totally displace Pr^{3+} from the *exo* face. Spectra were taken within 10 min after each addition of the drug. The addition of TMP caused a slight broadening of the upfield ^{31}P signal but did not result in the upfield movement of the *endo* ^{31}P resonance expected if Pr^{3+} were being displaced. Equilibration of the sample for 24 hr did not result in any further changes in the spectrum. These results indicate TMP does not passively permeate the membrane bilayer. Examination of each of the derivatives in Table 2 revealed that increasing the lipophilicity of TMP does not result in the ability to displace Pr^{3+} from the *endo* face of the membrane bilayer. Thus, although derivatization results in an increase in membrane binding, it does not promote membrane permeation.

Conclusions

TMP can be divided at the benzylic methylene into a hydrophilic (2,4-diaminopyrimidine) and a hydrophobic (3′,4′,5′-trimethoxybenzyl) residue. The molecule thus possesses a molecular amphiphilic moment (35) that runs along an axis extending from 2- to the 4′-carbon. When TMP moves into a polarity gradient such as that at the membrane interface, the amphiphilic moment should experience a torque that would tend to orient the molecule perpendicular to the membrane surface and parallel to zones of equal hydrophobicity. The proposed mechanism of binding via penetration of the hydrophobic 3′,4′,5′-trimethoxybenzyl moiety into the nonpolar fatty acid region of the membrane and placement of the polar 2,4-diaminopyrimidine ring in the lipid headgroup region is in

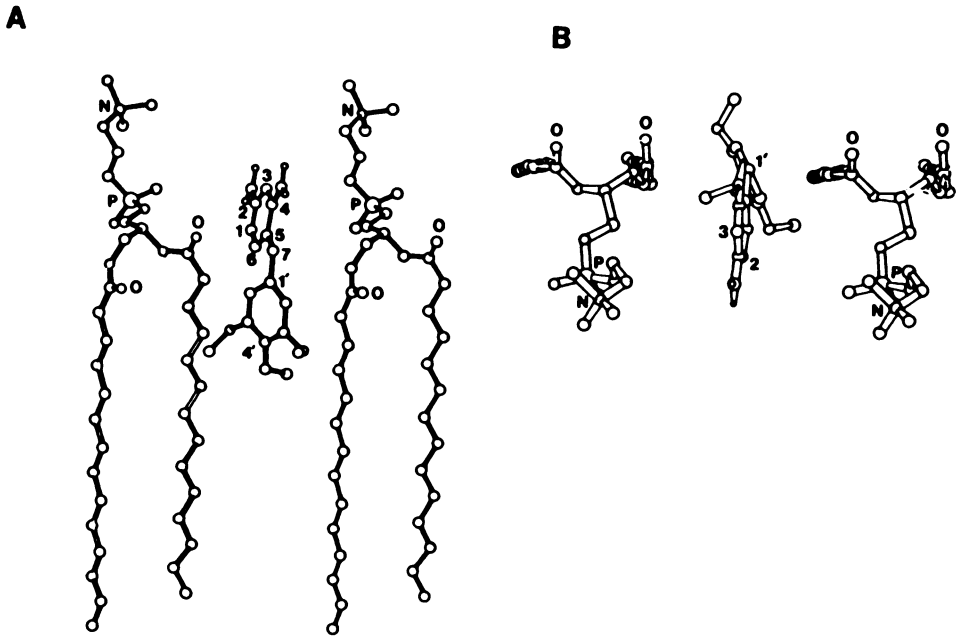

Fig. 5. A ball-and-stick model of one possible orientation of TMP relative to two adjacent DMPC molecules of a membrane bilayer viewed from the side (A) and above (B). The atoms of the TMP molecule are numbered and selected atom types on the DMPC molecule are labeled. The rotational axis of the 3′,4′,5′-trimethoxybenzyl group can be positioned parallel to the axes of the fatty acid chains of the membrane lipids, while the 2,4-diaminopyrimidine moiety can be placed simultaneously in the polar headgroup region near the phosphate-binding site of Pr^{3+}. The TMP is in a minimum energy conformation for the isolated molecule in the gas phase. Crystallographically determined coordinates (36) were used to construct the three-dimensional computer model of a DMPC bilayer. Space in the phospholipid matrix for intercalation of TMP was created by removing a single DMPC molecule from the bilayer model.

accord with the alignment of the molecular amphiphilic moment. The pyrimidine ring can interact with residual water in this interfacial location, retaining its aqueous solvation sphere. As illustrated in the hypothetical arrangement in Fig. 5, the conformation of TMP is well suited for this type of amphiphilic binding. The molecule can be inserted into a hole in the membrane lattice so that the accessible surface area available for van der Waals interaction between the benzyl moiety and the lipid fatty acid chains is maximized. Substitution of lipophilic chains at the 4′-position can increase contact between the drug and the lipid fatty acid chain, since in the antiperiplanar conformation the axis of the 4′-substituent can lie parallel to the axis of the fatty acid chain. Substitution at the 3′-position does not have the potential for such a favorable interaction geometry.

The insufficiency of *C* log *P* as a predictor of the membrane binding efficiency of TMP derivatives (see Table 2) may be explained in terms of both the enthalpic and entropic components of the total membrane binding energy. The lipophilicity of TMP (as indicated by *C* log *P*) is increased by increasing the size and complexity of the 3′- or 4′substituent (see Table 1). As the molecular volume of the substituted 5-benzyl moiety is increased by placing a substituent in either the 3′- or 4′-position, a greater free volume is required in the membrane phospholipid matrix for intercalation. The enthalpic cost of forming a larger space in the bilayer may partially offset any potential gains in complex stability due to increased van der Waals contact area. In addition, the entropic cost of the molecule assuming a conformation(s) in which the surface contact area for interaction with lipid fatty acids is maximized goes up as the number of free rotors in the 3′- or 4′-substituent increases. The gauche+, gauche−, *trans* approximation was used to calculate the number of conformational options, *W*, available to each of the TMP derivatives (37) (Table 2). Conformations exhibiting severe nonbonded interactions were eliminated. As the length of the chain is increased, the number of conformational options increases geometrically and the subset of the geometric space that allows favorable van der Waals interaction with the membrane bilayer becomes a smaller portion of the total conformational space. Thus, entropic considerations may partially explain why the order of membrane binding is the inverse of that predicted on lipophilic considerations alone.

We attribute the lack of permeability observed for TMP to the high energy required for breaking hydrogen bonds between the hydrogen bond donors (2-amino, 4-amino) and acceptors (N1, N3) on the pyrimidine ring and extravesicular water. A theory of the diffusion of nonelectrolytes across thin lipid membranes has been proposed in which the bilayer leaflet is envisioned to be a series of energy barriers, one at each interface between the membrane and the media and a number of them inside (38). To overcome the interfacial energy barrier and enter the membrane, each hydrogen-bonding interaction anchoring the permeant molecule in the aqueous phase must be broken, a step which increases the value of $\Delta H\ddagger$ for formation of the first transition state by an average of 5 kcal/mol (39). This translates to a reduction in the transfer rate to the first transition state of 6- to 10-fold per hydrogen bonding interaction. TMP has six hydrogen bonding interactions with water that result in a substantial barrier for movement of the 2,4-diaminopyrimidine across the membrane interface.

The mechanism of interaction between TMP and the model DMPC bilayer proposed here should be general for any phospholipid bilayer. Thus, it is unlikely that TMP can cross the cytoplasmic membrane by passive diffusion. The binding of the drug to the phospholipid matrix of the vesicle is consistent with the observed concentration of TMP in membranes during fractionation experiments. In biomembranes this interaction is undoubtedly augmented by binding to integral membrane proteins (40). Having ruled out passive diffusion as a mechanism by which TMP can enter cells, we are investigating alternative transport mechanisms. The availability of TMP to cytoplasmic DHFR may be mediated by a process similar to but much less efficient than that proposed for the 5,6-disubstituted 2,4-diaminopyrimidines in which the drug first binds to the membrane and is then extracted into the cytoplasm by binding to intracellular protein. Alternatively, a specific endogenous protein may function as a low efficiency carrier.

Acknowledgments

The authors thank Dr. Lee Kuyper for providing us with [2-^{13}C]trimethoprim, Webb Andrews for assisting with molecular modeling studies, Terry Fairley for making the viscosity measurements, and Professor Ned Porter for his suggestions and criticisms throughout this work.

References

1. Bertino, J. R., and D. G. Johns. Folate antagonists, in *Cancer Chemotherapy II* (I. Brodsky and S. B. Kohn, eds.). Grune and Stratton Inc., New York, 9–22 (1972).
2. Bushby, S. R. M., and G. H. Hitchings. Trimethoprim, a sulphonamide potentiator. *Br. J. Pharmacol. Chemother.* **33**:79–90 (1968).
3. Hakala, M. T. Transport of antineoplastic agents, in *Handbook of Experimental Pharmacology* (A. C. Sartorelli and D. G. Johns, eds.), Vol. 38. Springer-Verlag, Berlin, 240–269 (1974).
4. Goldman, I. D., N. S. Lichenstein, and V. T. Oliverio. Carrier-mediated transport of the folic acid analogue methotrexate in the L1210 leukemia cell. *J. Biol. Chem.* **243**:5007–5017 (1968).
5. Hill, B. T., L. A. Price, S. I. Harrison, and J. H. Goldie. Studies on the transport and distribution of diaminopyrimidines in L5178Y lymphoblasts in cell culture. *Biochem. Pharmacol.* **24**:535–538 (1975).
6. Niethammer, D., and R. C. Jackson. Transport of folate compounds through the membrane of human lymphoblastoid cells, in *Chemistry and Biology of Pteridines* (W. Pfleiderer, ed.). Walter de Gruyter, Berlin, 197–207 (1975).
7. Greco, W. R., and M. T. Hakala. Cellular pharmacokinetics of lipophilic diaminopyrimidine antifolates. *J. Pharmacol. Exp. Ther.* **212**:39–46 (1978).
8. Roth, B., E. Aig, B. S. Rauckman, J. Z. Strelitz, A. P. Phillips, R. Ferone, S. R. M. Bushby, and C. W. Sigel. 2,4-Diamino-5-benzylpyrimidines and analogues as antibacterial agents. 5. 3′,5′-Dimethoxy-4′-substituted-benzyl analogues of trimethoprim. *J. Med. Chem.* **24**:933–941 (1981).
9. Tritton, T. R., S. A. Murphee, and A. C. Sartorelli. Characterization of drug-membrane interactions using the liposome system. *Biochem. Pharmacol.* **26**:2319–2323 (1977).
10. Fischer, J. J., and O. Jardetzky. Nuclear magnetic relaxation study of intermolecular complexes. The mechanism of penicillin binding to serum albumin. *J. Am. Chem. Soc.* **87**:3237–3244 (1965).
11. Cresswell, R. M., J. W. Mentha, and R. L. Seaman. U.S. Patent No. 3,697,512 (1972).
12. Ames, B. N., and D. T. Dubin. The role of polyamines in the neutralization of bacteriophage deoxyribonucleic acid. *J. Biol. Chem.* **235**:769–775 (1960).
13. Shaka, A. J., J. Keller, and R. Freeman. Evaluation of a new broadband decoupling sequence: WALTZ-16. *J. Magn. Reson.* **53**:313–340 (1983).
14. Freeman, R., and H. D. W. Hill. Fourier transform study of NMR spin-lattice relaxation by "progressive saturation." *J. Chem. Phys.* **54**:3367–3377 (1969).
15. Hanssum, H. Optimization of fast inversion-recovery Fourier transform experiments. *J. Magn. Reson.* **45**:461–465 (1981).
16. Cory, M., D. MeKee, J. Kagan, D. W. Henry, and J. A. Miller. Design, synthesis, and DNA binding properties of bifunctional intercalators. Comparison of polymethylene and diphenyl ether chains connecting phenanthridine. *J. Am. Chem. Soc.* **107**:2528–2536 (1985).
17. Ogina, T., G. I. Shulman, M. J. Avison, S. R. Gullans, J. A. den Hollander, and R. G. Shulman. 23Na and 39K NMR studies of ion transport in human erythrocytes. *Proc. Natl. Acad. Sci. USA* **82**:1099–1103 (1985).
18. Pike, M. M., S. R. Simon, J. A. Balschi, and C. S. Springer. High-resolution NMR studies of transmembrane cation transport. *Proc. Natl. Acad. Sci. USA* **79**:810–814 (1982).
19. Inagaki, F., and T. Miyazawa. NMR analyses of molecular conformations and conformational equilibria with the lanthanide probe method, in *Progress in Nuclear Magnetic Resonance Spectroscopy*, J. W. Emsley, J. Feeney, and L. H. Sutcliffe, eds.), Vol. 14. Pergamon Press, Oxford, 67–112 (1982).

20. Cotton, F. A., and G. Wilkinson. *Advanced Inorganic Chemistry: A Comprehensive Text*, Ed. 3. Wiley-Interscience, New York, 1056–1076 (1972).
21. Singh, M., J. J. Reynolds, and A. D. Sherry. Lanthanide induced shift and relaxation studies of aqueous L-proline solutions. *J. Am. Chem. Soc.* **105**:4172–4177 (1982).
22. Bassfield, R. L. The interaction of lanthanide shift reagents with cationic sites: A ^{1}H and ^{13}C NMR study of the solution geometry of nicotine *N*-methiodide. *J. Am. Chem. Soc.* **105**:4168–4172 (1983).
23. Huang, C., and J. T. Mason. Geometric packing constraints in egg phosphatidylcholine vesicles. *Proc. Natl. Acad. Sci. USA* **75**:308–310 (1978).
24. Seydel, J. K., and O. Wassermann. NMR-studies on the molecular basis of drug-induced phospholipidosis-II. Interaction between several amphiphilic drugs and phospholipids. *Biochem. Pharmacol.* **25**:2357–2364 (1976).
25. Jardetzky, O., and G. C. K. Roberts. *NMR in Molecular Biology*. Academic Press, New York, 329–416 (1981).
26. Doddrell, D., V. Glushko, and A. Allerhand. Theory of nuclear Overhauser enhancement and ^{13}C-^{1}H dipolar relaxation in proton decoupled carbon-13 NMR spectra of macromolecules. *J. Chem. Phys.* **56**:3683–3689 (1972).
27. Cheung, H. T. A., M. S. Searle, J. Feeney, B. Birdsall, G. C. K. Roberts, I. Kompis, and S. J. Hammond. Trimethoprim binding to *Lactobacillus casei* dihydrofolate reductase: a ^{13}C NMR study using selectively ^{13}C-enriched trimethoprim. *Biochemistry* **25**:1925–1931 (1986).
29. Cotton, F. A., V. W. Day, E. E. Hazen, Jr., and S. Larsen. Structure of methylguanidinium dihydrophosphate. A model compound for arginine-phosphate hydrogen bonding. *J. Am. Chem. Soc.* **95**:4834–4840 (1973).
29. Roth, B., and J. Z. Strelitz. The protonation of 2,4-diaminopyrimidines. I. Dissociation constants and substituent effects. *J. Org. Chem.* **34**:821–829 (1969).
30. Fernandez, M., and J. Cerbon. The importance of the hydrophobic interactions of local anesthetics in the displacement of polyvalent cations from artificial lipid membranes. *Biochim. Biophys. Acta* **183**:466–475 (1969).
31. Kitamura, K., T. Kishino, and K. Hozumi. Interaction of chlorpromazine hydrochloride with lecithin vesicles by the use of carbon-13 nuclear magnetic resonance. *Chem. Pharm. Bull. (Tokyo)* **25**:1264–1267 (1979).
32. Yeagle, P. L., W. C. Hutton, and R. B. Martin. Molecular dynamics of the local anesthetic tetracaine in phospholipid vesicles. *Biochim. Biophys. Acta* **465**:173–178 (1977).
33. Cerbon, J. NMR evidence for the hydrophobic interaction of local anesthetics. *Biochim. Biophys. Acta* **290**:51–57 (1972).
34. Kitamura, K., H. Kano, K. Yoneyama, and K. Hozumi. ^{1}H nuclear magnetic resonance study on transbilayer permeation of chlorpromazine in lecithin vesicles. *Mol. Pharmacol.* **20**:124–127 (1981).
35. Schwyzer, R. Estimated conformation, orientation, and accumulation of dynorphin A-(1-13)-tridecapeptide on the surface of neutral lipid membranes. *Biochemistry* **25**:4281–4286 (1986).
36. Pearson, R. H., and I. Pascher. The molecular structure of lecithin dihydrate. *Nature (Lond.)* **281**:499–501 (1979).
37. Flory, P. J. *Statistical Mechanisms of Chain Molecules*. Interscience Publishers, New York, 55–61 (1969).
38. Davison, H., and J. F. Danielli. *The Permeability of Natural Membranes*, Ed. 2. Cambridge University Press, Cambridge, England, 310–340 (1952).
39. Stein, W. D. *Theoretical and Experimental Biology*. Vol. 6: *The Movement of Molecules across Cell Membranes*. Academic Press, New York, 65–90 (1967)
40. Nichol, C. A., J. C. Cavallito, J. L. Woolley, and C. W. Sigel. Lipid-soluble diaminopyrimidine inhibitors of dihydrofolate reductase. *Cancer Treat. Rep.* **61**:559–564 (1977).

Send reprint requests to: Dr. George R. Painter, The Wellcome Research Laboratories, Burroughs Wellcome Co., 3030 Cornwallis Road, Research Triangle Park, NC 27709.